JOURNAL OF SOLID STATE CHEMISTRY 21, 91–98 (1977)

The Fe–Se System. III. Mössbauer Diffusional Line-Broadening Studies of Iron Selenide of Composition $Fe_{0.96}Se$

ARTHUR T. HOWE AND TOSHIHIDE TSUJI*

Department of Inorganic and Structural Chemistry, University of Leeds, Leeds LS2 9JT, England

Received November 8, 1976

Mössbauer diffusional broadening of the ^{57}Fe resonance has been observed in $Fe_{0.96}Se$ between 900 and 1003°K. The line shapes could not be fitted to a single Lorentzian peak, and area comparisons implied the presence of extended wings in the resonance, indicating non-Lorentzian peak shapes. The shapes are sensitive to the dimensionality of the jump pathway, and were analyzed, using the theory of Howe and Morgan, in terms of the one-, two-, and three-dimensional pathways possible in the NiAs-type structure. The results, taken in conjunction with previous tracer results on $Fe_{1-x}S$, indicated a mixed process, with a predominance of jumping along one dimensional pathways. The diffusion coefficient was in the region of 10^{-11} to 10^{-12} m^2 sec^{-1} at 973°K.

We have extended our high-temperature Mössbauer studies of the Fe–Se phase to compositions close to the stoichiometric limit, where x is small in $Fe_{1-x}Se$. Above 731°K the phase extends from FeSe to just beyond $Fe_{0.75}Se$ (Fe_3Se_4) (*1–3*). The NiAs-type structure is adopted for most of the phase above this temperature with the possibility of CdI_2-type ordering at high vacancy concentrations (*2*, *4*). In Part II we reported the observation of diffusional line-broadening in the Mössbauer spectra of samples of composition $Fe_{1.50}Se_2$ and $Fe_{1.55}Se_2$ (in the vicinity of Fe_3Se_4) at temperatures between 820 and 980°K (*5*). The present studies were undertaken to investigate the effects on the diffusion parameters of a reduction in the vacancy concentration. Our previous studies of diffusional line-broadening in $Fe_{1-x}O$ showed very little dependence of the broadening on vacancy concentration (*6*), which was interpreted in terms of vacancy clustering effects (*7*).

There is no published data concerning the diffusion parameters of any of the transition-metal selenide systems, apart from Part II of our studies (*5*). Compounds having the NiAs–CdI_2 structure are of interest in the area because of their very rapid metal atom diffusion rates, as found using tracer studies in $Ni_{1-x}S$ (*8*), $Fe_{1-x}S$ (*9*), using NMR in Na_xTiS_2 (*10*), or using Mössbauer spectroscopy in $Fe_{1.33}Te_2$ (*11*) and $Fe_{1+x}Se_2$ (*5*). Mössbauer studies hold the prospect of differentiating between the several possible jump types within these anisotropic structures, by use of the theory developed by Howe and Morgan (*12*). The results presented in Part II have been interpreted in this light.

Experimental

The experimental procedure was similar to that used in previous studies (*5*). Prereduced iron, enriched with ^{57}Fe, was combined with prereduced selenium in accurately known proportions to give $Fe_{0.96 \pm 0.01}Se$. The ground material (70 mg) was sealed in a silica capsule and placed in the boron nitride holder of a Ricor furnace. The temperature was controlled to within 0.2°K. Mössbauer

* On leave from the Faculty of Nuclear Engineering, Nagoya University, Japan.

ISSN 0022-4596

spectra were obtained as described in Part II (*5*) using a triangular waveform. The source-to-counter distance was larger than previously used, which reduced the geometrical effect to approximately 0.02% of the total number of counts. The spectra were folded, eliminating the influence of the geometrical effect in comparison to even the weakest sample absorption of 0.2% at 1003°K. The spectra were computer-fitted to the sum of Lorentzian peaks. Isomer shifts are with respect to iron at 295°K as zero. For the spectra obtained at 900–1000°K, a small doublet, having fixed parameters determined from a blank run, was included in the fits to represent the iron impurity in the aluminum furnace windows, as previously described (*5*).

Because of the small absorption (ca. 0.2%) of the iron selenide spectra at the highest temperatures used (973 and 1003°K) counting times sometimes extended to 6 weeks for one spectrum, and the entire series of runs took 9 months to complete. Within this period reproducibility of the high-temperature spectra was checked, and no changes were observed. There was never any evidence from the spectra of Fe_2SiO_4, which would be formed if traces of oxygen existed in the sample (*11*), and an upper figure of 0.01 at% oxygen in the sample can be deduced. The room temperature spectrum was the same before and after the runs. Microscopic investigation of the powder after the runs showed that only slight sintering had occurred, and that the particles, most of which were not plate-like, were essentially randomly oriented.

Evidence regarding the phase diagram around the stoichiometric composition (*1*, *2*) indicates that the NiAs-type region extends to FeSe ($x = 0$) only above 731°K. Above this temperature, and in the region of our measurements, the NiAs-type structure is retained for values of x up to or even larger than 0.21 in $Fe_{1-x}Se$. Our sample therefore has the NiAs-type structure (random distribution of cation vacancies) at the temperatures of diffusional broadening.

Below 731°K stoichiometric FeSe disproportionates into $Fe_{1.04}Se$ and $Fe_{1-x}Se$ (*1*, *2*), where the value of x increases at lower temperatures and is approximately 0.12 at room temperature. The room-temperature spectrum was consistent with the expected mixture of $Fe_{1.04}Se$ and $Fe_{1-x}Se$, and exhibited two overlapping paramagnetic spectra. The spectrum of $Fe_{1.04}Se$ was reported in Part I (*13*). Our studies of $Fe_{1-x}Se$ at temperatures below 731°K will be reported in a later publication. The evidence is in agreement with the recent room temperature Mössbauer studies of $Fe_{1-x}Se$ at compositions on the iron-rich side of the Fe_7Se_8 subphase (*14*, *15*).

Results

Following a series of preliminary spectra which defined the temperature range of interest, long runs were performed at 773, 873, 923, 943, 949, 958, 973, and 1003°K. Up to 873°K the spectrum was a single peak with a full width at half-maximum (fwhm) of approximately 0.5 mm sec^{-1}. Above 873°K the intensity of the absorption dropped dramatically with increasing temperature, accompanied by an increase in the fwhm. The three spectra shown in Fig. 1, taken at 873, 973, and 1003°K,

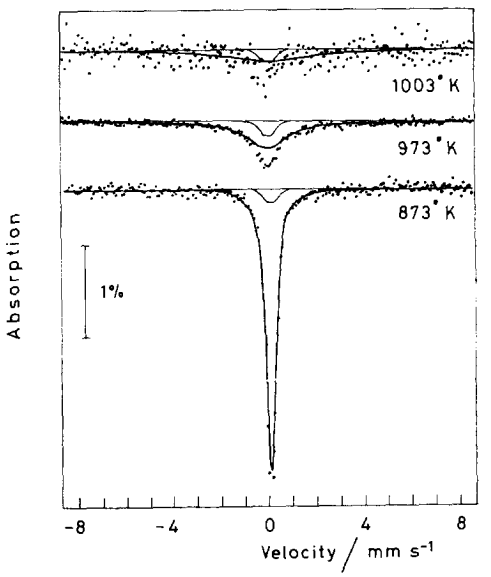

FIG. 1. Mössbauer spectra of $Fe_{0.96}Se$. The broadening is evident at the two higher temperatures. The small doublet from the furnace windows (shown) has been subtracted from the data to give the selenide spectra, shown as the solid lines.

illustrate these changes, which we attribute to diffusional effects. The temperature of the melting point ca. 1300°K (*3*) is so much higher than these temperatures that premelting phenomena could not provide an explanation.

For diffusional broadening in the NiAs-type lattice, Howe and Morgan (*12*) have shown that the lineshape is dependent upon the types of jump pathways, which have been previously illustrated (*5*, *12*). Jumping in a one-dimensional pathway, perpendicular to the planes of metal atoms and in the *c* direction, termed ε-type jumping, produces highly cusped non-Lorentzian spectra. Jumping in a two-dimensional pathway parallel to the metal atom planes, α-type jumping, produces less cusped spectra. Finally, jumping in a three-dimensional pathway, δ-type jumping results in spectra which are only slightly different from a Lorentzian shape.

The spectra, in the light of this knowledge, were first tested for the goodness of fit of a Lorentzian shape. The two small overlapping peaks from the iron in the windows were represented by fixed parameters (intensities of 0.11% for each peak), as determined from a blank run and described in Part II (*5*). The overall least-squares fits were only partially satisfactory, as can be seen from the sums of residuals given in Table 1. The curves for the selenide alone (total fit minus the impurity peaks) are shown in Fig. 1.

Fits to two Lorentzian peaks, plus the fixed impurity doublet, yielded marginally improved χ^2 values, as can be seen from Table 1. The two peaks had fwhm of 1.48 and 30 mm sec^{-1} at 973°K. This fit is shown in Fig. 2. It can be considered to be an approximate least-squares fit to the data, revealing wings, which are evident in the figure, extending to high and low velocities. Allowing the parameters of the impurity peaks to float, or even omitting them completely, did not alter these conclusions or provide better overall fits.

TABLE I

χ^2 VALUES FOR ALTERNATIVE FITS TO THE SPECTRA OF $Fe_{0.96}Se$ WITH 249 OR 252 DEGREES OF FREEDOM, RESPECTIVELY

Temperature (°K)	943	949	958	973	1003
χ^2 One peak fit	295	314	297	316	258
χ^2 Two peak fit	289	291	280	272	—

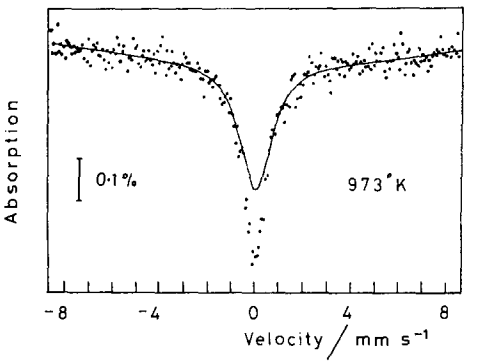

FIG. 2. Mössbauer spectrum of $Fe_{0.96}Se$ at 973°K. The doublet from the furnace windows has been subtracted from the fit to the original data to give the least-squares fit to the selenide spectrum (shown as the line).

However, there is no theoretical significance to the two Lorentzian components (*12*), and the two peaks have merely been used as a convenience to obtain a net least-squares fit to the expected non-Lorentzian data, represented by the line in Fig. 2. In fact, the parameters of the component Lorentzians themselves were unrealistic. The broad peak reproduced the wings of the spectrum by fitting the entire 256 channels to the flat-bottomed tip of the peak. This resulted in the very large fwhm of 30 mm sec^{-1} at 973°K, and, in addition, the baseline became an entirely artificial one. The result was that the area of the broad peak was unrealistically large. This situation is in contrast to that found for $Fe_{1.50}Se_2$ and $Fe_{1.55}Se_2$, where the two component Lorentzians satisfactorily accounted for the area behavior. For these samples, however, the values of χ^2 were lower than in the present study.

The importance of the wings in the description of the total resonance is dramatically shown when the peak areas are considered. Figure 3 shows the fwhm, absorption, and area (as the product of these two values) obtained from the one-peak fits after accounting for the impurity doublet. The central portion of the resonance, described approxi-

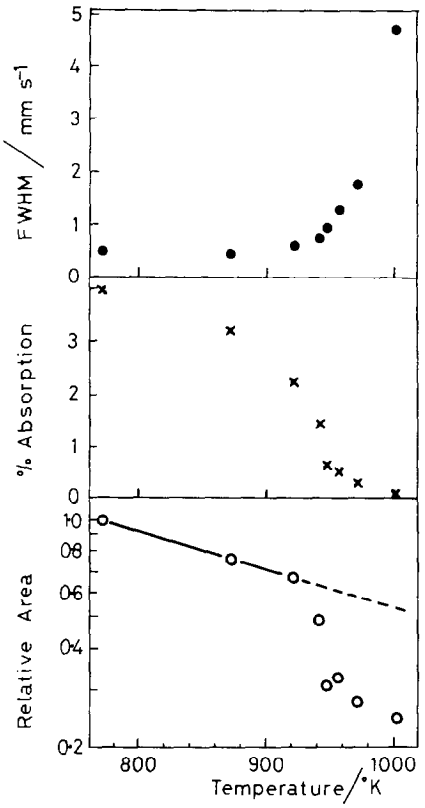

FIG. 3. Full width at half-maxima (FWHM), percentage absorption and relative area of a one-peak fit to the data of $Fe_{0.96}Se$ as a function of temperature. While the central portion of the resonance can be described approximately by one peak, failure to consider the broad wings shows up as an incorrect drop in the area when broadening occurs.

mately by the one Lorentzian peak, shows a sharp increase in the fwhm, and a decrease in the intensity, at the higher temperatures. Before the onset of diffusional broadening, the logarithm of the area was linear with temperature, as expected from the Debye–Waller expression. Knauer (*16*) showed that this relationship should extend unaltered into the diffusion broadening regime, and this was indeed shown to be the case for $Fe_{1.50}Se_2$ and $Fe_{1.55}Se_2$. Apart from small desaturation effects, the areas of the broadened resonances of $Fe_{0.96}Se$ should therefore extend the straight-line plot. This is seen not to be the case, and at 1003°K the area represented by the Lorentzian peak is only about one half that of the expected area. The difference must be made up by the wings of the resonance.

Discussion

For the case of the NiAs-type structure, where the cation vacancies are not ordered, the expressions of Howe and Morgan (*12*) simplify to give Lorentzian cross sections for any particular angle the γ ray makes with the direction of jumping in a single crystal. The Mössbauer absorption cross section is given by

$$\sigma_a(E) = \frac{\sigma_0 \Gamma \pi}{\hbar} \exp(-2W_a)\, S(\mathbf{k}\omega),$$

where Γ is the experimental fwhm in the absence of broadening; W_a is the Debye–Waller factor and

$$S = \frac{1}{\pi}\left(\frac{\frac{\Gamma}{2\hbar} + X - Y}{\omega^2 + \left(\frac{\Gamma}{2\hbar} + X - Y\right)^2}\right).$$

These expressions are obtained from the general expressions (*12*) by equating the subscript 1 with the subscript 2 terms. Further,

$$X - Y = \bar{\alpha}\left(1 - \frac{f(\mathbf{k})}{6}\right) + \bar{\varepsilon}\left(1 - \cos\frac{(\mathbf{k}\cdot\mathbf{c})}{2}\right) + \bar{\delta}\left(1 - \frac{1}{3}\cos\left(\frac{\mathbf{k}\cdot\mathbf{c}}{2}\right) - \tfrac{1}{9} f(\mathbf{k}) \cos\left(\frac{\mathbf{k}\cdot\mathbf{c}}{2}\right)\right),$$

where $f(\mathbf{k}) = \sum_{nn} \cos(\mathbf{k}\cdot\mathbf{r}_{nn})$, the sum over nearest neighbors. The average jump frequencies are related to the actual jump frequencies defined earlier through the fraction of metal atom sites occupied, N. Thus

$$\bar{\alpha} = 6\alpha(1 - N), \qquad \bar{\varepsilon} = 2\varepsilon(1 - N),$$
$$\text{and} \qquad \bar{\delta} = 18\delta(1 - N).$$

When the Lorentzian cross sections are summed over all solid angles non-Lorentzian cross sections result (*12*), some of which have very wide wings. The shapes of these curves can be quantified by comparing the ratios of the relative intensities to the fwhm. The three lines in Fig. 4 have been constructed from simulated spectra. The room temperature lattice parameters obtained by Hirone and

Chiba (*1*) for iron-rich $Fe_{1-x}Se$ ($a = 354.8$, $c = 573.3$ pm) were used. The simulated spectra were insensitive to small changes in the lattice parameters such as might occur with temperature or composition effects, and for this reason the lines are the same as for the disordered case of $Fe_{1.55}Se_2$ shown in Part II. The intensities are expressed as fractions of the intensity in the absence of diffusion. The fwhm in this case was taken to be the experimental fwhm of the peak at 873°K (0.488 mm sec^{-1}), which is the same to within experimental error as the minimum fwhm for $Fe_{1.55}Se_2$ (0.484 mm sec^{-1}). The areas of all the simulated curves were the same.

In order to plot the experimental points on such a graph the intensities and fwhm of the least-squares fits to the data are required. As we have shown for our sample, the shapes are not Lorentzian. The intensities will be slightly larger and the fwhm will also be slightly larger than the one-peak fit to the data due to the broad wings. However the difference between the two intensities will not be greater than the statistical uncertainty of the data, otherwise a very high χ^2 value would result from the simple Lorentzian fits. It is therefore safe to use the Lorentzian parameters to obtain approximate points on the plot, and these are shown in Fig. 4. The intensities have been expressed as a fraction of the intensities which would have been found at the same temperature in the absence of broadening. These values were obtained using a straight-line extrapolation of the data obtained below 900°K.

The error bars in Fig. 4 are the sums of (a) the maximum correction due to the presence of the wings, as just discussed; (b) the standard deviations obtained from the fits; and (c) an estimated possible correction for desaturation effects. Trial fits using different values of the intensity of the doublet due to iron in the aluminum windows, which constituted only an appreciable correction at the higher temperatures, only shifted the points parallel to the α-type line in Fig. 4. The experimental points can therefore be placed, with a high degree of confidence, in the middle section between the two extreme lines, rather than near the ε-type line or the δ-type line.

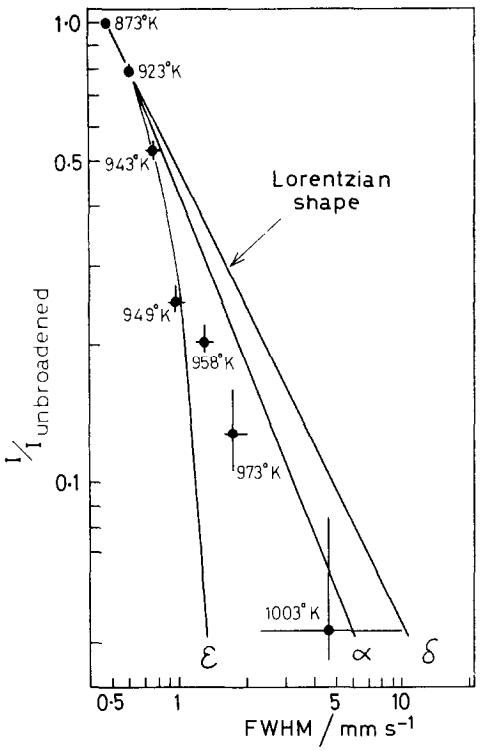

FIG. 4. Relative intensity as a function of FWHM of simulated spectra (lines) and the experimental spectra (points). The line for δ-type jumping is almost identical to Lorentzian behavior.

Since the δ-type line corresponds closely to Lorentzian behavior, the plot confirms the non-Lorentzian character of the resonances.

Now since the points do not follow any of the three lines exactly, suggestive of a mixed conduction pathway, we explored the effect of mixed pathways by simulating families of lines for various jump frequency combinations of ε, α, and δ. It was found that small admixtures of α- or δ- to ε-jump types reduced the non-Lorentzian character of the cross sections considerably. For instance, when ε and α were such that $D_{zz}/D_{xx} = 2$, the plot, for various jump frequencies, lay between the pure α and pure δ lines in Fig. 4, indicating a nearly Lorentzian peak-shape. Jumping in both the z direction (ε-type), and in the x–y plane (α-type) has therefore resulted in behavior resembling the three-dimensional jumping.

The positions of the experimental points in Fig. 4 are therefore consistent with the two following interpretations:

(a) ε-type jumping contributes mainly to the line-broadening, with the presence of α, or δ, or both types of jumping modifying the line shape in the direction of Lorentzian behavior,

(b) The broadening is caused by predominantly α-type jumping. The experimental points do not fall directly on the α-line in Fig. 4, but the error bars for most of the points extend to near the α region, and this interpretation could not altogether be excluded.

The broadening could not be caused by a predominance of δ-type jumping.

The line broadening can be related more directly to the diffusion coefficients than to the actual jump frequencies. Now the probability that an atom, starting at an origin at time $t = 0$, will be at the point r at a later time t, $G_s(rt)$, is proportional to the jump frequency if the motion is random, or upon f times the jump frequency for nonrandom motion in the limit of large values of r. f is the Bardeen–Herring correlation factor (*17*), and equals unity for random-walk jumping. Both the Mössbauer line broadening and the diffusion coefficients depend on $G_s(rt)$, the former over all values of r and the latter in the limit of large r. Hence the broadening can be considered to be approximately scaled down by the correlation factor (*18*), and to a first approximation the dependence of the line shape on jump pathway will not be substantially changed. In a similar way the diffusion coefficients are scaled down by the correlation factors, thus

$$D_{xx} = D_{yy} = \frac{a^2}{4}(f_\alpha \bar{\alpha} + \tfrac{2}{3} f_\delta \bar{\delta}),$$

$$D_{zz} = \frac{c^2}{2}(f_\varepsilon \bar{\varepsilon} + f_\delta \bar{\delta})$$

for the case of the disordered NiAs-type structure, where a and c are the lattice parameters.

The correlation factors have been considered by Condit, Hobbins, and Birchenall (*9*). For ε-type jumps it was shown that f_ε could be very low, and for exclusive ε-type jumping both the Mössbauer line broadening and the tracer diffusion coefficients would be lower than otherwise expected. However the correlation factors for α- and δ-type jumping would lie in the range 0.6 to 0.8, and line broadening would imply jump rates close to those given by the simple equations we have used.

Although a knowledge of the operative jump pathways is required before the diffusion coefficients or activation energies can be calculated from the Mössbauer line broadening, some estimate can be gained by doing the calculation for some of the possible mechanisms. The values of the respective diffusion coefficients so obtained were in the region of 10^{-11} to 10^{-12} m^2 sec^{-1} at 973°K. Assuming a predominance of ε-type jumping, an activation energy in the region of 200 kJ mole^{-1} was deduced.

It is of interest to compare the results obtained for $Fe_{0.96}Se$ with the two tracer studies of the isostructural $Ni_{1-x}S$ (*8*) and $Fe_{1-x}S$ (*9*), where x was small in both cases. The jump distances, at room temperature, for $Ni_{1-x}S$, $Fe_{1-x}S$, and $Fe_{1-x}Se$ for ε-type jumping ($c/2$) and for α-type jumping (a) are, respectively, 265 and 343, 286 and 345, 286 and 353 pm. δ-type jump distances are greater than these values. The ratio of the diffusion coefficients in the c and a direction, D_{zz}/D_{xx}, was found to be 1.4 in $Ni_{1-x}S$ and 1.9 in $Fe_{1-x}S$, both values being reasonably independent of x over the ranges studied. Judging from the larger a parameter of $Fe_{1-x}Se$, one would expect a higher value of D_{zz}/D_{xx} in this compound. This could only occur if either ε- or δ-type jumping were predominant over α-type jumping. Such an argument would rule out one possible interpretation of the Mössbauer data which was in terms of predominantly α-type jumping. The Mössbauer results would therefore suggest that ε-type jumping was responsible for diffusion in the z direction, rather than δ-type jumping. The inclusion of correlation effects would not be expected to alter this conclusion.

Comparing the results obtain from $Fe_{0.96}Se$ with those obtained for $Fe_{1.50}Se_2$ and $Fe_{1.55}Se_2$, we see that

(a) Line broadening begins below 900°K

for all compositions. The onset temperature was higher for $Fe_{0.96}Se$ (ca. 900°K) than for the more nonstoichiometric samples (ca. 800°K). Assuming that the mechanism did not change, the results indicate a higher activation energy for diffusion in $Fe_{0.96}Se$ than for the other samples.

(b) The shapes of the respective Mössbauer resonances were all non-Lorentzian. Those of $Fe_{0.96}Se$ could not be approximated well by two superimposed Lorentzian peaks, whereas those of the other two samples could. However, an analysis of all the shapes could be made in terms of the same jump pathways.

The changes in the line broadening in going from $Fe_{0.96}Se$ to $Fe_{1.50}Se_2$ were therefore not marked, and could possibly disguise changes in the jump frequencies of up to a factor of 10 if the jump pathways altered in relative magnitude to one another. (See Fig. 4, ref. 12 for the different sensitivities of the broadening to the jump types). Associated with the composition change has been an increase, by a factor of about six, of the concentration of vacancies, and also a decrease in the c lattice parameter, at room temperature, from 573 to 559 pm, while the a spacing was constant. In addition, as the vacancy concentration increases, the f factors would be expected to increase due to the increased possibility of an atom having two or more adjacent vacancies. These three factors would all result in larger diffusion coefficients for $Fe_{1.50}Se_2$ than for $Fe_{0.96}Se$. However, the structure of $Fe_{1.50}Se_2$ is that of the CdI_2-type even up to 977°K (*2*). Here the vacancies are ordered into every second cation layer, indicative of a larger vacancy–vacancy repulsion between adjacent sites in the z direction than in the xy direction. The interaction energies, in $Ni_{1+x}Te_2$, are of the order of 20 kJ mole^{-1} (*19*). Such an additional contribution to an activation energy of jumping of 100 kJ mole^{-1} would reduce the jump rate by a factor of approximately three at 1000°K. It can be seen that these above considerations adequately describe the behavior of the Fe–Se system, since our experimental results are within the range of variation suggested by these factors.

Detailed consideration of such factors has been given to the composition dependence of the tracer diffusion coefficients of $Fe_{1-x}S$ in order to try and distinguish between, for instance, ε- and δ-type jumping. Condit, Hobbins, and Birchenall (*9*) considered the f factors in detail, and their dependence on mechanism and defect concentration. However an explanation of the results could not be arrived at without considering vacancy repulsion effects. This was considered in more detail by Murch, Rolls, and de Bruin (*20*), who were able to reproduce the experimental trends by assuming that vacancy repulsions extended to 32 surrounding sites, and that ε-type jumping was of most importance compared to δ-type jumping. Although these results are corroborated by our findings, one would like to have seen account taken of the variations in the f factors with vacancy concentration, which was not done due to the complications involved. The study of Mössbauer line broadening in single crystals holds the prospects of providing direct information regarding the jump pathways in anisotropic materials, and such experiments are planned for the future.

References

1. T. Hirone and S. Chiba, *J. Phys. Soc. Japan* **11**, 666 (1956).
2. F. Grønvold, *Acta Chem. Scand.* **22**, 1219 (1968).
3. S. R. Svendsen, *Acta Chem. Scand.* **26**, 3757 (1972).
4. A. Okazaki and K. Hirakawa, *J. Phys. Soc. Japan* **11**, 930 (1956).
5. T. Tsuji, A. T. Howe, and N. N. Greenwood, *J. Solid State Chem.* **20**, 287 (1977).
6. N. N. Greenwood and A. T. Howe, *J. Chem. Soc. Dalton* 122 (1972).
7. N. N. Greenwood and A. T. Howe, *in* "Proc. Seventh Int. Symp. on the Reactivity of Solids" (J. S. Anderson, F. S. Stone, and L. M. Roberts, Eds.) p. 240, Chapman and Hall, London (1972)
8. S. M. Klotsman, A. N. Timofeyev, and I. Sh Trakhtenberg, *Fizk. Metall.* **17**, 132 (1964), (*Phys. Metals Metallogr.* **17**, 119 (1964)).
9. R. H. Condit, R. R. Hobbins, and C. E. Birchenall, *Oxid. Metals* **8**, 409 (1974).
10. B. G. Silbernagel and M. S. Whittingham, *Mat. Res. Bull.* **11**, 19 (1976).
11. A. T. Howe, P. Coffin, and B. E. F. Fender *J. Phys. C: Solid State Phys.* **9**, L61 (1976).

12. A. T. HOWE AND G. J. MORGAN, *J. Phys. C: Solid State Phys.* **9**, 4463 (1976).
13. T. TSUJI, A. T. HOWE, AND N. N. GREENWOOD, *J. Solid State Chem.* **17**, 157 (1976).
14. K. B. LAL, S. MENDIRATTA, AND G. N. RAO, *Phys. Status Solidi (a)* **32**, K79 (1975).
15. K. V. REDDY AND S. C. CHETTY, *Phys. Status Solidi (a)*, **32**, 585 (1975).
16. R. C. KNAUER, *Phys. Rev. B* **3**, 567 (1971).
17. J. R. MANNING, "Diffusion Kinetics for Atoms in Crystals," Van Nostrand, Princeton, N.J., (1971).
18. G. J. MORGAN, private communication.
19. P. COFFIN, A. J. JACOBSON, AND B. E. F. FENDER, *J. Phys. C: Solid State Phys.* **7**, 2781 (1974).
20. G. E. MURCH, J. M. ROLLS, AND H. J. DE BRUIN, *Philos. Mag.* **29**, 337 (1974).